Environ. Sci. Technol. **2004**, *38,* 4542−4548

Protection of Mesopore-Adsorbed Organic Matter from Enzymatic Degradation

ANDREW R. ZIMMERMAN,*,†,§
JON CHOROVER,‡
KEITH W. GOYNE,‡ AND
SUSAN L. BRANTLEY†

Department of Geosciences, The Pennsylvania State University, University Park, Pennsylvania 16802, and Department of Soil, Water and Environmental Science, University of Arizona, Tucson, Arizona 85721

Synthetic mesoporous alumina and silica minerals with uniform pore geometries, and their nonporous analogues, were used to test the role of mineral mesopores (2−50 nm diameter) in protecting organic matter from enzymatic degradation in soils and sediments. Dihydroxyphenylalanine (L-DOPA), a model humic compound, was irreversibly sorbed to both mineral types. The surface area-normalized adsorption capacity was greater for the mesoporous minerals relative to their nonporous analogues. The degradation kinetics of free and mineral-sorbed L-DOPA by the enzyme laccase was monitored in a closed cell via oxygen electrode. Relative to freely dissolved L-DOPA, nonporous alumina-sorbed substrate was degraded, on average, 90% more slowly and to a lesser extent (93%), likely due to laccase adsorption to alumina. In contrast, relative to free L-DOPA, degradation of nonporous silica-sorbed L-DOPA was enhanced by 20% on average. In the case of mesoporous alumina and silica-sorbed L-DOPA, the enzyme activity was 3−40 times lower than that observed for externally sorbed substrate (i.e., L-DOPA sorbed to nonporous minerals). These results provide strong evidence to support the viability of the mesopore protection mechanism for sequestration and preservation of sedimentary organic matter and organic contaminants. Nanopore adsorption/desorption phenomena may aid in explaining the slow degradation of organic contaminants in certain soils and sediments and may have implications for environmental remediation and biotechnological applications.

Introduction

Despite its lability, it has been observed that some fraction of biomolecular organic matter (OM) and degradable contaminants remain preserved in soils and sediments, apparently unavailable for microbial utilization (*1*, *2*). Direct correlations between organic carbon and specific surface area in many soils and sediments (*3*, *4*−*7*), and the slower mineralization of sorbed versus desorbed marine sedimentary OM (*8*) and soil OM (*9*), suggest that formation of OM−mineral complexes can stabilize labile forms of OM against microbial attack (*10*, *11*). The biodegradation and bioremediation of organic contaminants in soils are also retarded by mineral sorption (*12*, *13*). Organic contaminants have been found to become less bioavailable with "aging" time following initial adsorption (*14*, *15*). The processes responsible for this behavior within soils, sediments, and aquifers are not well understood.

Cycling of organic carbon in sediments and soils has been characterized by complex kinetics in which fast and slow processes of carbon degradation are observed (*2*). Fast cycling has been related to biodegradation of readily available OM, whereas slow cycling has been attributed to the occurrence of a less bioavailable portion of the OM. This dual availability character has been attributed both to recalcitrant versus labile fractions and to sorbed versus dissolved fractions (*8*, *16*). However, decreased biological degradation of organic compounds has also been attributed to the presence of pores in soils and test materials (*14*, *17*, *18*). Because mineral surface areas can be dominated by the internal surfaces of pores ranging 2−50 nm in diameter (*19*, *20*), some workers have suggested that mineral mesopores play a major role in the sequestration and preservation of sedimentary OM (*19*, *21*). This may occur by physical occlusion of OM within mineral pores, thus protecting OM from degradative attack by bacteria and their extracellular enzymes (*19*, *21*, *22*). Others have even suggested that OM sorption to soil minerals may be a prerequisite to mineralization because of the preferential colonization of surfaces by microorganisms (*23*). Here, we directly test the viability of the "mesopore protection" hypothesis with in vitro combinations of either mesoporous or nonporous mineral analogues and a model organic substrate−enzyme pair.

In our initial tests of the mesopore protection hypothesis, amino acid monomers and polymers were sorbed onto and desorbed from fabricated mesoporous and nonporous alumina and silica in batch aqueous experiments (*24*). Each mineral pair was of similar surface chemistry (site density and charge properties) and differed only in the presence or absence of intraparticle mesoporosity (*25*). All amino acid monomers and polymers smaller than about one-half of the pore diameter exhibited significantly greater surface area-normalized adsorption to mesoporous alumina and silica as compared to nonporous analogues. Proteins of sizes similar to or larger than the mesopores exhibited diminished adsorption to porous relative to nonporous solids, indicating sorptive exclusion from the internal pore surfaces. Further, evidence for enhanced retention of OM within mesopores was found in the increased desorption hysteresis for mesoporous versus nonporous mineral-sorbed amino acid compounds. Although the mechanism of pore affinity remains unclear, it is plausible that a unique chemical environment exists therein (e.g., electric double layer overlap or water exclusion), to favor stronger sorption. Nonetheless, the observation—that small organic molecules may be strongly retained in mesopores whereas enzyme-sized molecules may be excluded—suggests the protective capacity of mesopores.

The goal of this study was to directly test the mesopore protection hypothesis by comparing the enzyme-mediated degradation rate of an organic compound sorbed to nonporous versus mesoporous minerals. A diphenol, 3,4-L-dihydroxyphenylalanine (L-DOPA), was chosen as a model small organic compound as it possesses moieties commonly found in complex natural OM and phenolic xenobiotics

* Corresponding author phone: (352)392-0070; fax: (352)392-9294; e-mail: azimmer@geology.ufl.edu.
† The Pennsylvania State University.
‡ University of Arizona.
§ Present address: University of Florida, Department of Geological Sciences, 241 Williamson Hall, P.O. Box 112120, Gainesville, FL 32611-2120.

10.1021/es035340+ CCC: $27.50

Published on Web 07/23/2004

(carboxylic, amine, hydroxyl). L-DOPA was incubated with laccase, a member of the phenoloxidase class of enzymes that are capable of catalyzing the oxidation of aromatic compounds using molecular oxygen (*26*). Although the particular laccase used was derived from *Trametes villosa* fungi, many soil microorganisms including bacteria and other fungi are known to produce phenoloxidases (*27*). The results indicate that small organic molecules are not accessible to enzymatic degradation when sorbed within mineral mesopores, and, therefore, we provide direct evidence for the viability of the proposed mineral mesopore protection mechanism for sequestration and preservation of natural and contaminant organic compounds.

Materials and Methods

Mineral Sorbents. Amorphous mesoporous alumina (Al_2O_3) and silica (SiO_2) minerals were synthesized by the neutral template route as described by Komarneni et al. (*28*) and Pauly and Pinnavaia (*29*), respectively. Briefly, dodecylamine was stirred in water and ethanol while aluminum isopropoxide or tetraethyl orthosilicate was slowly added (0.27:29.6:9.09:1.0 and 0.25:127.5:10.3:1.0 molar ratios, for alumina and silica, respectively). After 20 h of aging (while stirred at 65 °C in the case of silica) followed by air-drying, the material was calcined (540 °C, 6 h) to remove the organic template leaving only the inorganic support. Mesoporous alumina and silica were of unimodal pore size distribution with mean pore diameters of 8.2 and 4.0 nm, respectively, and specific surface areas of 242 and 962 $m^2\ g^{-1}$, respectively, as determined by N_2 sorptometry. On the basis of N_2 sorptometry, we also estimate that 96.5% and 99.7% of the fabricated alumina and silica surface area, respectively, is located within pores between 2 and 20 nm in size (*25*).

Nonporous alumina (γ-Al_2O_3) and silica, with specific surface areas of 37 and 7.5 $m^2\ g^{-1}$, respectively, were purchased from Alfa Aesar (Ward Hill, MA; stock Nos. 40007 and 89709, respectively) and were chosen for their similarity in surface charge properties to their mesoporous analogues. Following washing of the nonporous alumina (0.02 M $CaCl_2$, 24 h, 5 times), all minerals, porous as well as nonporous, were found to be free of organic carbon, that is, below detection limits. All were used as powders with particle sizes of roughly 0.1 μm. Additional information on the morphology and chemistry of the sorbents is published elsewhere (*24*, *25*).

Sorption and Desorption Methods. L-DOPA (Sigma-Aldrich; St. Louis, MO) was used as received and reacted with mesoporous and nonporous minerals in an aqueous batch suspension, as described previously (*24*). Briefly, surface area-normalized batch reactions were conducted by adding 80 m^2 of mineral to 50 mL polypropylene centrifuge tubes containing 25 mL of aqueous background solution (0.02 M $CaCl_2$, and 200 mg L^{-1} $HgCl_2$ as a bactericide). A pH of 6.5 was maintained by addition of HCl for alumina, and $Ca(OH)_2$ for silica minerals. After 3 d of end-over-end rotation at 8 rpm, tubes were centrifuged (4500 rpm, 1 h), the supernatant solution was removed and replaced with 25 mL of OM-free background solution, and the particles were redispersed on an agitator for 1 min prior to a 3 d desorption period with the same rotational mixing. The surface excess (sorbed μmol) of L-DOPA and its change during desorption were calculated from the difference between L-DOPA concentration in a sorbent-free control and that of the suspension supernatant solution. L-DOPA concentrations were measured on a fluorometer after the addition of a fluorescent derivative (*30*). Laccase adsorption isotherms were determined similarly except a 5 min adsorption period was used (to match the time period of enzyme experiments, below) and solution concentrations were measured using a Bio-Rad protein assay (UV detection at 595 nm), calibrated with albumin standards.

Enzyme Activity Assays. Fungal-derived extracellular laccase (*T. villosa*, EC 1.10.3.2) was provided by Novo Nordisk (Danbury, CT). The activity of laccase, with free and adsorbed L-DOPA as substrate, was determined using a biological oxygen monitor (BOM model 5300; Yellow Spring Instruments Co., Yellow Springs, OH) equipped with a Clark oxygen electrode (5357 Oxygen Probe; Yellow Spring Instruments Co.). Mineral-sorbed L-DOPA was prepared and quantified as above. After L-DOPA adsorption, minerals were rinsed in 5 mL of background electrolyte solution for 5 min to remove the easily desorbable fraction, and the mass of sorbate retained was calculated. Five milliliter aliquots of dissolved L-DOPA solution, or varying masses of mineral with sorbed L-DOPA and 5 mL of background solution, were then sealed without air bubbles into the BOM sample chamber and incubated at 25 °C while stirring with a Teflon-coated magnetic bar. After the vessel was sealed and the oxygen probe was equilibrated, 0.1 mL of laccase solution (15 μg mL^{-1}) was introduced through a side port next to the electrode via syringe. Oxygen concentration in the vessel was recorded every 30 s until oxygen consumption ceased, after no more than 5 min in all cases. Following incubations, sorbents from BOM vessels were transferred quantitatively into preweighed pans, dried (80 °C), and weighed to record the mass of sorbent material so that the mass of sorbed L-DOPA present in the reactor could be calculated.

Using energy minimization modeling techniques (*24*) and other published sources, we estimate the spherical molecular diameters of laccase (66 kDa) (*31*) and L-DOPA to be about 7 and 0.5 nm, respectively. Thus, on the basis of our previous findings (*24*), we expect that L-DOPA will be able to enter both alumina and silica mesopores (8.2 and 4.0 nm mean diameters, respectively) and laccase will largely be excluded from the pores.

Data Analysis. Adsorption data were fit to the Langmuir−Freundlich (LF) isotherm that takes the form

$$q = \frac{NbC^{m}}{1 + bC^{m}} \tag{1}$$

and describes the equilibrium relationship between the surface excess of sorbate, q, and the equilibrium concentration of adsorptive in solution, C (*32*). N, b, and m are fitting parameters that represent adsorption maximum, affinity, and site heterogeneity, respectively. The LF equation is useful when modeling adsorption of organic compounds to energetically heterogeneous materials (*32*, *33*). The LF isotherm equation was fit to the experimental data following the method of Umpleby et al. (*33*) in which the solver function of Microsoft Excel 2002 is used to maximize the coefficient of determination (R^2) through iterative variation of the fitting parameters. R^2 is calculated from the sum of residuals, that is, the difference between experimental and model-predicted values of q. Methods used to calculate a hysteresis index are detailed elsewhere (*24*).

The kinetics of the conversion of free (i.e., dissolved) L-DOPA to the product dopaquinone (Figure 3, inset 1) was modeled by the Michaelis−Menten equation

$$v_o = \frac{V_{max}S_o}{S_o + b} \tag{2}$$

where S_o, v_o, and V_{max} are the initial substrate concentration, the initial reaction rate, and the maximum initial reaction rate, respectively. Systems obeying Michaelis−Menten kinetics are linear when S_o and v_o are plotted in double-reciprocal form. This Lineweaver−Burk plot has an intercept of $1/V_{max}$ and a slope of K_m/V_{max} where K_m is the so-called half-saturation constant or substrate affinity.

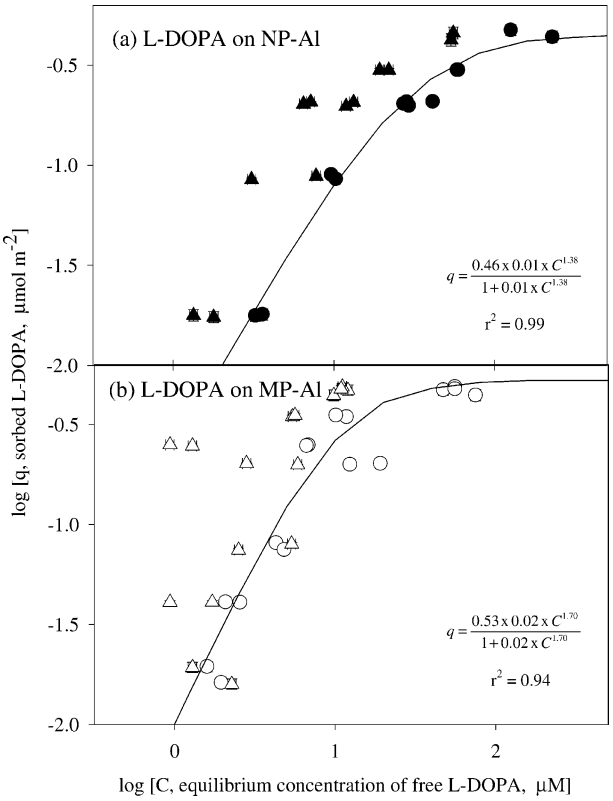

FIGURE 1. L-DOPA adsorption/desorption to (a) nonporous alumina (filled symbols), and (b) mesoporous alumina (open symbols). Adsorption data are shown as circles, and desorption data are shown as triangles. Error bars represent 95% confidence intervals for each data point. Lines are best-fit Langmuir−Freundlich isotherms (equations shown) for adsorption data only.

Results

Substrate Adsorption−Desorption. The adsorption−desorption of L-DOPA on nonporous and mesoporous alumina (NP−Al and MP−Al, respectively) and silica (NP−Si and MP−Si, respectively) sorbents were similar to that of amino acid monomers and dimers investigated previously (*24*). First, adsorption isotherm data were not well-fit by the common Langmuir and Freundlich equations but were better predicted by the hybrid LF eq 1 (Figures 1 and 2). Second, adsorption maxima, *N*, expressed on a surface area-normalized basis, were similar or greater for mesoporous versus nonporous mineral analogues (0.53 and 0.46 μmol m^{-2} for MP−Al and NP−Al, respectively, and 1.29 and 0.07 μmol m^{-2}, for MP−Si and NP−Si, respectively). In addition, the mesoporous sorbents exhibited greater surface area-normalized adsorption at all equilibrium solution concentrations of adsorptive, *C*. The binding affinity, *b*, of L-DOPA was 2 times greater for MP−Al versus NP−Al but 3 times smaller for MP−Si versus NP−Si. Last, the magnitude of desorption hysteresis was greater for mesoporous versus nonporous mineral-sorbed L-DOPA (Figures 1 and 2); hysteresis indices (24) were 2 times (MP−Al) and 4 times (MP−Si) higher than those for the corresponding nonporous sorbents.

These sorption data highlight the unique nature of internal mesopore adsorption of small organic compounds as compared to those sorbed to external surfaces. Relatively strong adsorptive interaction and/or inhibited desorption of compounds from mesopores have been variously attributed to increased intramolecular interaction of sorbate molecules due to surface curvature (*34*), superposition of interaction potentials on opposing pore walls (*35*), electric double layer overlap (*36*), or pore-filling (*24*). Although the mechanism for enhanced adsorption to mesoporous minerals remains unclear, it is evident that L-DOPA and other small organic molecules can be strongly sorbed, sometimes irreversibly, to internal mesopore surfaces.

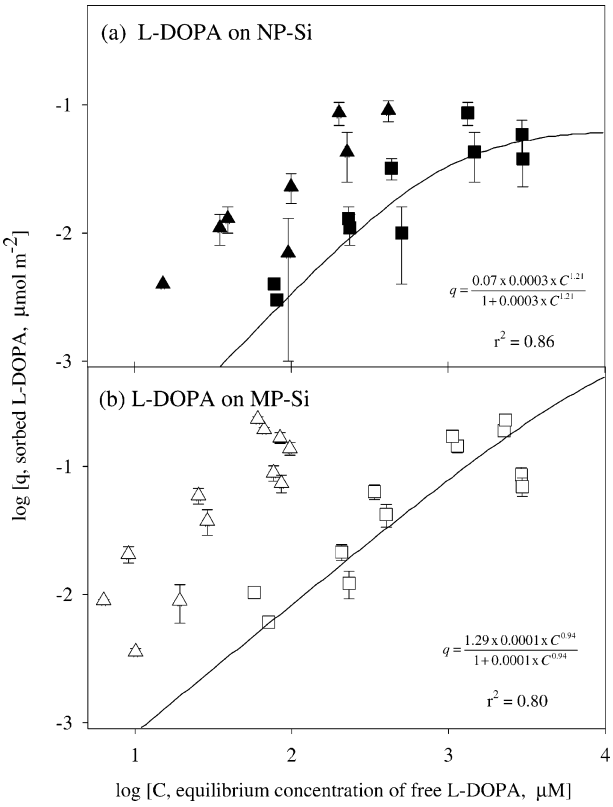

FIGURE 2. L-DOPA adsorption/desorption to (a) nonporous silica (filled symbols), and (b) mesoporous silica (open symbols). Other designations are the same as in the Figure 1 caption.

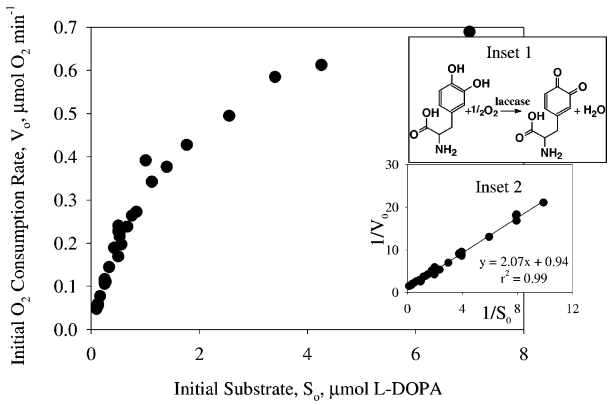

FIGURE 3. Kinetics of enzyme (laccase)-mediated conversion of free L-DOPA. Inset 1 shows the reaction. Inset 2 is the Lineweaver−Burk plot.

Substrate Incubations with Laccase. Conversion of free L-DOPA to the diketone product was well-modeled by eq 2, yielding V_{max} and K_m values of 1.06 μmol of O_2 consumed min^{-1} (stoichiometrically equivalent to 2.12 μmol of L-DOPA min^{-1}) and 2.20 μmol of L-DOPA, respectively (Figure 3). These kinetic constants are in the range of those reported for the conversion of L-DOPA or similar phenols by laccase or other phenoloxidases (*37*, *38*). The mass of L-DOPA present was linearly related to total O_2 consumption for free L-DOPA less than 1.5 μmol. We calculate that 0.77 (±0.07) mol of O_2 was consumed for each mole of dissolved L-DOPA present rather than the stoichiometrically predicted factor of 0.5 mol of O_2 mol^{-1} of L-DOPA. This may be because (i) the incubation

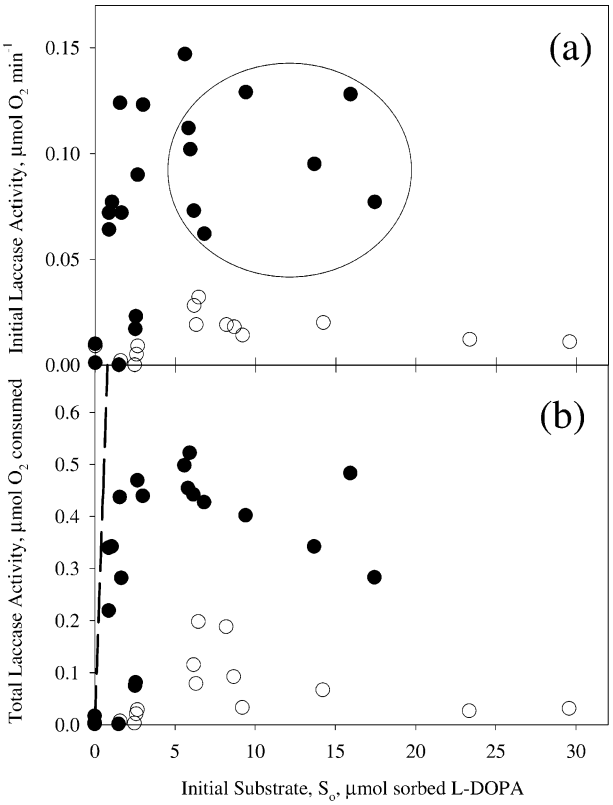

FIGURE 4. (a) Initial and (b) total activity of laccase-mediated degradation of L-DOPA sorbed to nonporous (closed symbols) and mesoporous (open symbols) alumina. Incubations displaying the greatest apparent degree of activity suppression (discussed in text) are circled. The dashed line is the regression line for the conversion of free dissolved substrate.

solution was not fully O_2 saturated, (ii) less than the total 5 mL of solution was in contact with the added laccase, or (iii) additional free substrate would have been converted had further time been allowed.

Relative to the rate and extent of solution-phase substrate conversion observed for free L-DOPA, incubations of laccase with alumina-sorbed L-DOPA (porous or nonporous) resulted in lower enzyme activity and less total substrate converted (Figure 4; Table 1). For example, whereas the half-saturation substrate amount of 2.2 μmol of L-DOPA resulted in an initial enzyme activity of 0.53 μmol of O_2 min^{-1}, the same mass of NP−Al-sorbed L-DOPA resulted in a maximum observed rate of 0.12 μmol of O_2 min^{-1}. Fractional loss of initial enzyme activity due to adsorption to NP−Al-sorbed L-DOPA varied from 4% to 34% (mean of 10%). The dashed line shown in Figure 4b is the regression line in the low concentration region of free dissolved substrate conversion. All data points underlie this line and therefore indicate reduced conversion. On average, the extent of conversion of NP−Al-sorbed L-DOPA was 7% that of free L-DOPA.

In contrast, the rates and extents of laccase conversion of NP−Si-sorbed L-DOPA (Figure 5; Table 2) were similar to or greater than values obtained for equivalent masses of free L-DOPA. On average, excluding the two incubations with the most sorbed L-DOPA, initial enzyme activity and total L-DOPA converted using NP−Si-sorbed substrate were both 1.2 times that of dissolved substrate. Enhanced enzyme activity of NP−Si-sorbed substrate is indicated by points above the dashed line in Figure 5b.

Sorption to mesoporous alumina and silica resulted in much lower rates and extents of enzyme-mediated substrate conversion relative to those observed for nonporous sorbents. At similar L-DOPA loadings, initial laccase activity (Figure 4a) was 5−27 times greater for NP−Al relative to MP−Al, and total laccase activity (Figure 4b) was 4−36 times greater. Rates (Figure 5a) and extents (Figure 5b) of conversion of NP−Si-sorbed L-DOPA were enhanced over their MP−Si-sorbed analogues to a similar degree (7−16 times for both). For both sets of sorbents, initial and total enzyme activity increased steeply with substrate loading, eventually reaching a maximum and then decreasing with even higher substrate loading. Plausible reasons for this convex upward curve and differences in laccase-mediated degradation as a function of mineral morphology are discussed in the following section.

TABLE 1. Enzyme Degradation of Alumina-Sorbed L-DOPA Experimental Data

mineral-sorbed L-DOPA (mmol)	mineral mass (g)	initial enzyme activity (μmol of O_2 min^{-1})	total consumed oxygen (μmol of O_2)
	Nonporous Alumina		
0.000	0.837	0.001	0.001
0.000	0.389	0.010	0.017
0.876	0.116	0.072	0.340
0.876	0.119	0.064	0.219
1.061	0.144	0.077	0.342
1.491	1.190	0.000	0.001
1.559	0.211	0.124	0.437
1.649	1.293	0.072	0.282
2.515	0.780	0.017	0.075
2.544	0.822	0.023	0.081
2.660	0.360	0.090	0.469
2.995	0.275	0.123	0.439
5.591	0.512	0.147	0.498
5.813	0.771	0.112	0.454
5.927	0.825	0.102	0.522
6.154	0.813	0.073	0.442
6.814	0.900	0.062	0.427
9.398	0.861	0.129	0.402
13.676	1.254	0.095	0.342
15.925	1.461	0.128	0.483
17.437	1.599	0.077	0.283
	Mesoporous Alumina		
0.000	0.128	0.009	0.017
0.000	0.255	0.001	0.004
1.584	0.160	0.002	0.007
2.470	0.250	0.000	0.003
2.580	0.143	0.005	0.021
2.652	0.137	0.009	0.029
6.172	0.126	0.028	0.115
6.305	0.131	0.019	0.079
6.459	0.108	0.032	0.198
8.192	0.135	0.019	0.188
8.670	0.143	0.018	0.092
9.191	0.108	0.014	0.033
14.217	0.170	0.020	0.067
23.349	0.279	0.012	0.027
29.580	0.348	0.011	0.031

Discussion

Enzymatic Degradation of Nonporous Mineral-Sorbed Substrate. The comparative enzymatic degradation of free versus adsorbed substrate is complicated by the possibility that the enzyme itself may become sorbed to the particle surfaces, which can affect its activity. Many studies have examined the kinetic properties of mineral-adsorbed enzymes. Early work in this area focused on layer silicate clays (*39*−*41*), while, more recently, mesoporous materials have attracted attention for possible biotechnology applications because of their ability to stabilize enzymes over longer time periods (*42*, *43*). In all of these studies, however, enzymes were adsorbed or reagent-immobilized on surfaces prior to substrate addition. Our work is, to our knowledge, the first to show examples of both reduced and enhanced enzyme activity for sorbed versus free substrate.

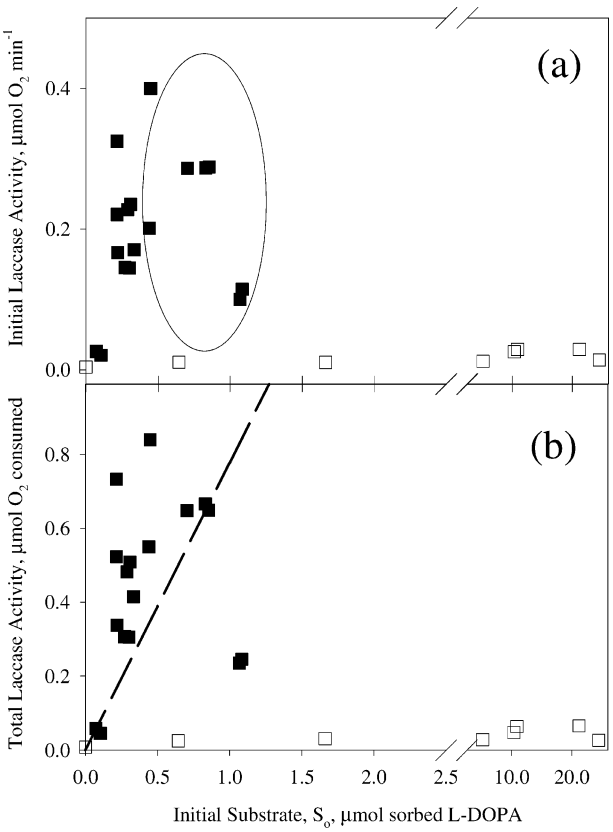

FIGURE 5. (a) Initial and (b) total activity of laccase-mediated degradation of L-DOPA sorbed to nonporous (closed symbols) and mesoporous (open symbols) silica. The circled data and dashed line are explained in Figure 4.

TABLE 2. Enzyme Degradation of Silica-Sorbed L-DOPA Experimental Data

mineral-sorbed L-DOPA (mmol)	mineral mass (g)	initial enzyme activity (μmol of O_2 min^{-1})	total consumed oxygen (μmol of O_2)
	Nonporous Silica		
0.072	2.587	0.026	0.059
0.104	3.733	0.021	0.045
0.216	2.664	0.325	0.733
0.216	2.664	0.221	0.523
0.220	1.493	0.166	0.338
0.270	1.834	0.145	0.307
0.290	2.413	0.228	0.482
0.303	2.054	0.145	0.306
0.309	2.575	0.235	0.509
0.334	4.120	0.171	0.415
0.439	3.662	0.201	0.550
0.449	3.045	0.400	0.840
0.704	2.438	0.286	0.647
0.832	2.880	0.287	0.666
0.855	2.960	0.288	0.649
1.067	6.135	0.100	0.235
1.084	3.440	0.115	0.246
	Mesoporous Silica		
0.000	0.093	0.004	1.335
0.645	0.103	0.011	0.025
1.661	0.116	0.011	0.031
5.140	0.125	0.012	0.028
10.348	0.125	0.026	1.339
10.877	0.163	0.029	1.334
21.179	0.116	0.029	1.338
24.467	0.111	0.014	1.359

Most workers have shown decreased enzyme activity (lower V_{max} and higher K_m, i.e., reduced substrate affinity) due to enzyme interaction with mineral surfaces (*44*). For example, the activity of acid phosphatase sorbed to montmorillonite and Al hydroxide was found to be reduced relative to its free activity by 80% and 65%, respectively (*44*). Likewise, the residual activity of different laccases adsorbed to several types of bentonite, kaolinite, and quartz was found to be reduced by 0−89%, 50−70%, and 43−65%, respectively (*39*). These reductions in enzyme activity may be attributable to steric hindrance, conformational changes of the enzyme induced by adsorption to the mineral surface (*40*), or pH changes close to the mineral surface that alter enzyme activity (*39*).

Cases of unchanged or increased enzyme activity upon mineral interaction, such as those that we observed for silica, are less common in the literature, although some have been noted (*41*). For example, Claus and Filip (*39*) observed little change in peroxidase and tyrosinase (both phenoloxidases) activity upon adsorption to quartz sand (residual activities of 106% and 101%, respectively). Many studies have examined reagent-immobilized enzymes on mesoporous silicas, and, in most cases, enzyme activity is lost (*45*, *46*). However, Lei et al. (*47*) documented that the activity of entrapped organophosphorus hydrolase was twice that of the free enzyme. It is possible that silica binds L-DOPA in such a way as to make it more accessible to enzymatic degradation. However, due to its associated H^+ ions, the pH is likely lower, closer to the negatively charged silica surface than in the bulk solution (*48*). We therefore hypothesize that enhanced laccase activity for NP−Si-sorbed versus free substrate may be because the pH is closer to the optimum pH for fungal laccase activity (i.e., pH 3−5) (*49*) close to silica's surface.

The kinetics observed in the mineral-sorbed L-DOPA systems cannot be modeled using the Michaelis−Menten equation. Instead, initial activity versus substrate curves for both nonporous minerals exhibit a hyberbolic shape and may be indicative of substrate inhibition. This is a special case of enzyme uncompetitive inhibition in which substrate molecules compete for active enzyme sites at high substrate concentrations (*50*). Our data fit the theoretical model describing substrate inhibition according to Cleland (*50*) and Whitwam and Tien (*51*) (see Supporting Information). However, this mechanism is unlikely because incubations at high substrate concentrations with no mineral present showed no evidence of declining enzyme activity. We note, however, that incubations displaying the greatest apparent degree of activity suppression (those circled in Figures 4a and 5a) were often those in which the greatest mineral surface area was added. For example, the eight NP−Al incubation data points circled in Figure 4a are among the 11 cases in which more than 0.81 g of mineral (>30 m^2) was used. Two other incubations using >30 m^2 of mineral resulted in almost no enzyme activity. Similarly, five of the six NP−Si incubations showing the greatest signs of activity suppression (circled in Figure 5a) are among the eight incubations with greater than 20 m^2 of mineral surface area added. We therefore hypothesize that suppressed laccase activity was due to laccase adsorption to mineral surfaces and this effect was greater in incubations with higher particle surface area.

To explore this hypothesis further, we conducted laccase adsorption experiments for each mineral phase using the same conditions as imposed during enzyme activity measurements. That is, a constant mass of laccase (1.5 μg) was added to 5 mL solutions with varying amounts of mineral for a period of 5 min. For each sorbent, plots of adsorbed laccase versus mineral surface area (Figure 6) were modeled using a simple exponential function, $q = k(\text{S.A.})^n$, where k and n are fitting parameters. The results indicate that at the conditions of the enzyme activity experiments, assuming no influence of mineral-sorbed L-DOPA, the majority (80−100%) of the laccase added was likely to have adsorbed to NP−Al

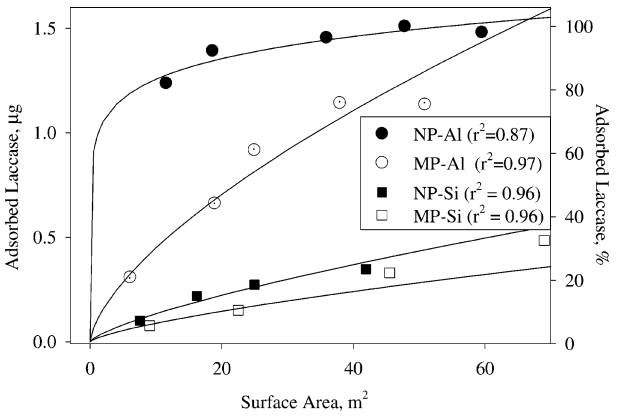

FIGURE 6. Laccase adsorption to alumina and silica minerals as a function of surface area. Lines are fits to an exponential model described in text.

where at least 10 m^2 of mineral surface area was present. Only 5−20% was likely to have sorbed to NP−Si. This may explain the greater suppression of laccase activity during experiments with alumina versus silica as well as the loss of enzyme activity in incubations with greater mineral surface area available for adsorption of laccase.

The above conclusion is also supported by prior reports. Suppression of montmorillonite-sorbed-tyrosinase activity, also a phenoloxidase, has been shown to vary directly with the degree of hydroxyaluminum coatings (*52*). Although ligand exchange and electrostatic and hydrophobic interactions are all considered important for protein-mineral adsorption (*53*−*55*), the former two are likely of greater importance for enzyme interaction with hydroxylated alumina surfaces and are, apparently, more apt to result in the observed enzyme activity suppression due to conformational changes.

Enzymatic Degradation of Mesoporous Mineral-Sorbed Substrate. While enzymatic degradation of L-DOPA was either somewhat reduced or enhanced by nonporous mineral adsorption, degradation was greatly reduced by adsorption to minerals with intraparticle mesoporosity. Importantly, the effect was present both for alumina, an activity-suppressing surface, and for silica, an activity-enhancing surface. This stronger suppression cannot be attributed to greater adsorption of laccase to the mesoporous minerals because, for both alumina and silica, the mesoporous materials were found to adsorb less laccase on a surface area-normalized basis (Figure 6). As an aside, it should be noted that under the adsorption conditions used, laccase covered only a small fraction (<0.01%) of the surfaces of the materials tested; thus, the effect of excluded mesoporous surface on adsorption reduction was not greater.

Another possibility is that L-DOPA was more readily desorbed from nonporous mineral surfaces during the incubations, leading to measurement of greater laccase activity. However, the amount of L-DOPA we would expect to desorb (10% and 30% maximum from alumina and silica, respectively, based on 3 d adsorption/desorption isotherms) could not support the observed differences in enzyme activity. The difference between substrate desorption from mesoporous versus nonporous analogues would be even smaller than the total desorbable fraction. Further, by rinsing the minerals prior to the start of the degradation experiment, the rapidly desorbing fraction was removed. These observations also argue against the oxidation of desorbed substrate having a strong effect on further desorption.

We therefore attribute the greater suppression of enzymatic activity in mesoporous systems to substrate occlusion within mesopores that are inaccessible to enzymes due to size and/or steric constraints. This is consistent with our previous finding that proteins of molecular dimensions similar to, or larger than, mesopore openings are inhibited from entering pores, resulting in lower surface area-normalized adsorption capacities (*24*). L-DOPA is of a molecular size (about 0.5 nm) likely to be sequestered within both the alumina and the silica mesopores (8.2 and 4.0 nm, respectively), while laccase (about 7 nm) was inhibited from entering most mesopores of both minerals.

Adsorption of organic compounds to mineral surfaces (*9*, *13*, *56*, *57*) and entrapment within intraparticle mineral pores (*12*, *14*, *17*, *57*) are believed to be responsible for the reduction of OM biodegradation rates in experiments conducted with live bacteria. Using enzymes and comparing nonporous and mesoporous minerals of similar surface chemistry, this study identifies a mechanism likely responsible for these observations. Although adsorption to mineral surfaces can enhance or retard enzymatic degradation of organic compounds, occlusion within nanometer-sized pores may lead to long-term preservation of even extremely labile OM and organic contaminants due to enzyme exclusion. We conclude that both the extent of enzyme adsorption to mineral surfaces and the degree of mineral nanoporosity are important factors in determining the likelihood of OM preservation in sediment and soil. Although this study utilizes a single enzyme−substrate system and synthetic minerals, it serves as a model from which studies utilizing more complex OM assemblages and mineral surface types may be extended. Furthermore, mesopore-adsorbed substrate systems may prove useful as delivery vehicles for organic compounds to agricultural, medical, or environmental systems.

Acknowledgments

We thank Drs. Sridhar Komarneni and Jean-Marc Bollag for use of their laboratories during mesoporous mineral synthesis and enzyme activity incubations, respectively. The laboratory assistance of Dr. Mi-Youn Ahn is especially appreciated. Acknowledgment is also made to the Penn State Biogeochemical Research Initiative for Education (BRIE) sponsored by NSF (IGERT) Grant DGE-9972759 and to the donors of the American Chemical Society Petroleum Research Fund for their support of this research.

Supporting Information Available

One figure showing Lineweaver−Burk plots and substrate inhibition models of enzyme activity. This material is available free of charge via the Internet at http://pubs.acs.org.

Literature Cited

(1) Hedges, J. I.; Keil, R. G. Sedimentary organic matter preservation: an assessment and speculative synthesis. *Mar. Chem.* **1995**, *49*, 81−115.

(2) Luthy, R. G.; Aiken, G. R.; Brusseau, M. L.; Cunningham, S. D.; Gschwend, P. M.; Pignatello, J. J.; Reinhard, M.; Traina, S. J.; Weber, W. J., Jr.; Westall, J. C. Sequestration of hydrophobic organic contaminants by geosorbents. *Environ. Sci. Technol.* **1997**, *31*, 3341−3347.

(3) Kennedy, M. J.; Pevear, D. R.; Hill, R. J. Mineral surface control of organic carbon in black shale. *Science* **2002**, *259*, 657−660.

(4) Bergamaschi, B. A.; Tsamakis, E.; Keil, R. G.; Eglinton, T. I.; Montlucon, D. B.; Hedges, J. I. The effect of grain size and surface area on organic matter, lignin, carbohydrate concentration, and molecular composition in Peru Margin sediments. *Geochim. Cosmochim. Acta* **1997**, *61*, 1247−1260.

(5) Mayer, L. M.; Macko, S. A.; Cammen, L. Provenance, concentration and nature of sedimentary organic nitrogen in the Gulf of Maine. *Mar. Chem.* **1988**, *25*, 291−304.

(6) Baldock, J. A.; Skjemstad, J. O. Role of soil matrix and minerals in protecting natural organic materials against biological attack. *Org. Geochem.* **2000**, *31*, 697−710.

(7) Zimmerman, A. R.; Canuel, E. A. Bulk organic matter and lipid biomarker composition of Chesapeake Bay surficial sediments as indicators of environmental processes. *Estuarine, Coastal Shelf Sci.* **2001**, *53*, 319−341.

(8) Keil, R. G. Sorptive preservation of labile organic matter in marine sediments. *Nature* **1994**, *370*, 549−552.
(9) Jones, D. L.; Edwards, A. C. Influence of sorption on the biological utilization of two simple carbon substrates. *Soil Biol. Biochem.* **1998**, *30*, 1895−1902.
(10) Kaiser, K.; Guggenberger, G. The role of DOM sorption to mineral surfaces in the preservation of organic matter in soils. *Org. Geochem.* **2000**, *31*, 711−725.
(11) Jastrow, J. D.; Miller, R. M. *Soil aggregate stabilization and carbon sequestration: Feedbacks through organo-mineral associations*; CRC Press: Boca Raton, FL, 1997; pp 207−223.
(12) Harms, H.; Zehnder, A. J. B. Bioavailability of sorbed 3-chlorodibenzofuran. *Appl. Environ. Microbiol.* **1995**, *61*, 27−33.
(13) Ogram, A. V.; Jessup, R. E.; Ou, L. T.; Rao, P. S. C. Effects of sorption on biological degradation rates of (2,4-dichlorophenoxy)acetic acids in soils. *Appl. Environ. Microbiol.* **1985**, *49*, 582−587.
(14) Steinberg, S. M.; Pignatello, J. J.; Sawhney, B. L. Persistence of 1,2-dibromoethane in soils: entrapment in intraparticle micropores. *Environ. Sci. Technol.* **1987**, *21*, 1201−1208.
(15) Hatzinger, P. B.; Alexander, M. Effect of aging of chemicals in soils on their biodegradability and extractability. *Environ. Sci. Technol.* **1995**, *29*, 537−545.
(16) Torn, M. S.; Trumbore, S. E.; Chadwick, O. A.; Vitousek, P. M.; Hendricks, D. M. Mineral control of soil organic carbon storage and turnover. *Nature* **1997**, *389*, 170−173.
(17) Nam, K.; Alexander, M. Role of nanoporosity and hydrophobicity in sequestration and bioavailability: Test with models. *Environ. Sci. Technol.* **1998**, *32*, 71−74.
(18) Shor, L. M.; Liang, W.; Rockne, K. J.; Young, L. Y.; Taghon, G. L.; Kosson, D. S. Intra-aggregate mass transport-limited bioavailability of polycyclic aromatic hydrocarbons to Mycobacterium strain PC01. *Environ. Sci. Technol.* **2003**, *37*, 1545−1552.
(19) Mayer, L. M. Relationships between mineral surfaces and organic carbon concentrations in soils and sediments. *Chem. Geol.* **1994**, *114*, 347−363.
(20) Chung, N.; Alexander, M. Relationship between nanoporosity and other properties of soil. *Soil Sci.* **1999**, *164*, 726−730.
(21) Mayer, L. M. Surface area control of organic carbon accumulation in continental shelf sediments. *Geochim. Cosmochim. Acta* **1994**, *58*, 1271−1284.
(22) Hulthe, G.; Hulth, S.; Hall, P. O. J. Effect of oxygen on degradation rate of refractory and labile organic matter in continental margin sediments. *Geochim. Cosmochim. Acta* **1998**, *62*, 1319−1328.
(23) Guggenberger, G.; Kaiser, K. Dissolved organic matter in soil: challenging the paradigm of sorptive preservation. *Geoderma* **2003**, *113*, 293−310.
(24) Zimmerman, A. R.; Goyne, K. W.; Chorover, J.; Komarneni, S.; Brantley, S. L. Mineral mesopore effects on nitrogenous organic matter adsorption. *Org. Geochem.* **2004**, *335*, 355−375.
(25) Goyne, K. W.; Zimmerman, A. R.; Newalkar, B. L.; Komarneni, S.; Brantley, S. L.; Chorover, J. Surface charge of variable porosity Al_2O_3 (s) and SiO_2(s) adsorbents. *J. Porous Mater.* **2002**, *9*, 243−256.
(26) Duran, N.; Esposito, E. Potential applications of oxidative enzymes and phenoloxidase-like compounds in wastewater and soil treatment: a review. *Appl. Catal., B* **2000**, *28*, 83−99.
(27) Gianfreda, L.; Bollag, J.-M. Isolated enzymes for the transformation and detoxification of organic pollutants. In *Enzymes and the environment: Activity, ecology, and applications*; Burns, R. G., Dick, R. P., Eds.; Marcel Dekker: New York, 2002; pp 495−538.
(28) Komarneni, S.; Pidugu, R.; Menon, V. Water adsorption and desorption isotherms of silica and alumina mesoporous molecular sieves. *J. Porous Mater.* **1996**, *3*, 99−106.
(29) Pauly, T. R.; Pinnavaia, T. J. Pore size modification of mesoporous HMS molecular sieve silicas with wormhole framework structures. *Chem. Mater.* **2001**, *13*, 987−993.
(30) Lindroth, P.; Mopper, K. High performance liquid chromatographic determination of subpicomolar amounts of amino acids by precolumn fluorescence derivitization with *o*-phthaldialdehyde. *Anal. Chem.* **1979**, *51*, 1667−1674.
(31) Yaropolov, A. I.; Skorobogat'ko, O. V.; Vartanov, S. S.; Varfolomeyev, S. D. Laccase. Properties, catalytic mechanism, and applicability. *Appl. Biochem. Biotechnol.* **1994**, *49*, 257−280.
(32) Sips, R. Structure of a catalyst surface. *J. Chem. Phys.* **1948**, *16*, 490−495.
(33) Umpleby, R. J.; Baxter, S. B.; Chen, Y.; Shah, R. N.; Shimizu, K. D. Characterization of molecularly imprinted polymers with the Langmuir-Freundlich isotherm. *Anal. Chem.* **2001**, *73*, 4584−4591.
(34) Goyne, K. W.; Chorover, J.; Zimmerman, A. R.; Komarneni, S.; Brantley, S. L. Influence of mesoporosity on the sorption of 2,4-dichlorophenoxyacetic acid to alumina and silica. *J. Colloid Interface Sci.* **2004**, *272*, 10−20.
(35) Farrell, J.; Reinhard, M. Desorption of halogenated organics from model solids, sediments, and soil under unsaturated conditions. 1. Isotherms. *Environ. Sci. Technol.* **1994**, *28*, 53−62.
(36) Wang, Y.; Bryan, C.; Xu, H.; Pohl, P.; Yang, Y.; Brinker, J. Interface chemistry of nanostructured materials: Ion adsorption on mesoporous alumina. *J. Colloid Interface Sci.* **2002**, *254*, 23−30.
(37) Sanchez-Amat, A.; Solano, F. A pluripotent polyphenol oxidase from the melanogenic marine *Altermonas* sp. shares catalytic capabilities of tyronsinases and laccases. *Biochem. Biophys. Res. Commun.* **1997**, *240*, 787−792.
(38) Akta, N.; Tanyola, A. Kinetics of laccase-catalyzed oxidative polymerization of catechol. *J. Mol. Catal. B* **2003**, *22*, 61−69.
(39) Claus, H.; Filip, Z. Behavior of phenoloxidases in the presence of clays and other soil-related adsorbents. *Appl. Microbiol. Biotechnol.* **1988**, 506−511.
(40) Naidja, A.; Huang, P. M.; Bollag, J.-M. Enzyme−clay interaction and their impact on the transformation of natural and anthropogenic organic compounds in soil. *J. Environ. Qual.* **2000**, *29*, 677−691.
(41) Boyd, S. A.; Mortland, M. Enzyme interactions with clays and clay-organic matter complexes. In *Soil Biochemistry*; Stotzky, G., Bollag, J.-M., Eds.; Marcel Dekker: New York, 1990; Vol. 6, pp 1−28.
(42) Wei, Y.; Xu, J.; Feng, Q.; Dong, H.; Lin, M. Encapsulation of enzymes in mesoporous host materials via the nonsurfactant-templated sol−gel process. *Mater. Lett.* **2000**, *44*, 6−11.
(43) Diaz, J. F.; Balkus, K. J., Jr. Enzyme immobilization in MCM-41 molecular sieve. *J. Mol. Catal. B* **1996**, *2*, 115−126.
(44) Rao, M. A.; Violante, A.; Gianfreda, L. Interation of acid phosphatase with clays, organic molecules and organo-mineral complexes: kinetics and stability. *Soil Biol. Biochem.* **2000**, *32*, 1007−1014.
(45) Brauna, S.; Rappoporta, S.; Zusmanb, R.; Avnirb, D.; Ottolenghi, M. Biochemically active sol−gel glasses: the trapping of enzymes. *Mater. Lett.* **1990**, *10*, 1−5.
(46) Li, T.; Li, L.; Zhao, J.; Gui, Z. Encapsulation of enzymes in mesoporous host materials via the nonsurfactant-templated sol−gel process. *Mater. Lett.* **2000**, *44*, 6−11.
(47) Lei, C.; Shin, Y.; Liu, J.; Ackerman, E. J. Entrapping enzyme in a functionalized nanoporous support. *J. Am. Chem. Soc.* **2002**, *124*, 11242−11243.
(48) Stumm, W.; Morgan, J. J. *Aquatic Chemistry*, 3rd ed.; John Wiley & Sons: New York, 1996.
(49) Gianfreda, L.; Xu, F.; Bollag, J.-M. Laccases: A useful group of oxidoreductive enzymes. *Biorem. J.* **1999**, *3*, 1−25.
(50) Cleland, W. W. Substrate Inhibition. In *Contemporary enzyme kinetics and mechanism*; Puich, D. L., Ed.; Academic Press: New York, 1983; Vol. 2, pp 253−266.
(51) Whitwam, R.; Tien, M. Heterologous expression and reconstitution of fungal Mn peroxidase. *Arch. Biochem. Biophys.* **1996**, *333*, 439−446.
(52) Naidja, A.; Huang, P. M.; Bollag, J.-M. Activity of tyrosinase immobilized on hydroxyaluminum-montomorillonite complexes. *J. Mol. Catal. A* **1997**, *115*, 305−316.
(53) Yoon, J.-Y.; Kim, J.-H.; Kim, W.-S. The relationship of interaction forces in the protein adsorption onto polymeric microspheres. *Colloids Surf., A* **1999**, *153*, 413−419.
(54) Arai, T.; Norde, W. The behavior of some model proteins at solid−liquid interfaces 1. Adsorption from single protein solutions. *Colloids Surf.* **1990**, *51*, 1−15.
(55) Servagent-Noinville, S.; Revault, M.; Quiquampoix, H.; Baron, M.-H. Conformational changes of bovine serum albumin induced by adsorption on different clay surfaces: FTIR analysis. *J. Colloid Interface Sci.* **1999**, *221*, 273−283.
(56) Marshman, N. A.; Marshall, K. C. Bacterial growth on proteins in the presence of clay minerals. *Soil Biol. Biochem.* **1981**, *13*, 127−134.
(57) Hatzinger, P. B.; Alexander, M. Biodegradation of organic compounds sequestered in organic solids or nanopores within silica particles. *Environ. Toxicol. Chem.* **1997**, *16*, 2215−2221.

Received for review December 2, 2003. Revised manuscript received May 11, 2004. Accepted May 18, 2004.

ES035340+